Progress In Electromagnetics Research B, Vol. 97, 73–89, 2022

Evaluation of Lightning Electromagnetic Induction on Buried Signaling Cable of High-Speed Railway Considering the Frequency Dependence of Soil Electrical Parameters

Yaqiong Qiao[1, 3], Zhiguo Liang[2, *], Longsheng Wang[2], Shuai Bai[2], Jianlei Gang[2], Hongyang Zhang[2], and Wu Duan[2]

Abstract—Evaluation of the lightning coupling on the buried signaling cable nearby when the through-ground wire is used as the discharge channel of lightning current requires accurate models for the calculation of the underground lightning electromagnetic field and the induced current of this field on the signaling cable conductor. To accomplish this, a full-wave approach based on the finite-element method (FEM) is used, which incorporates the frequency dependence of soil conductivity and relative permittivity into in the model. The numerical results show that for soils characterized by relatively low resistivity values (less than 4000 Ω·m), the frequency dependence of the electrical properties of the soil has a negligible influence on the horizontal component of the electric field and the vertical component of the magnetic field. However, the distribution of the lightning electromagnetic field is markedly affected by the distance between the air-soil interface and the buried signaling cable. We also find that the coupling strength of the lightning electromagnetic field to the buried signaling cable is strongly dependent on the wave shape of the lightning current, soil resistivity, the distance between the cable and the air-soil interface, and the distance between the cable and the lightning strike point. Finally, the common grounding methods of the cable shielding layer in cable protection are compared. Results show that single-layer double-terminal grounding is the most effective anti-interference measure for the electromagnetic field coupling between the through-ground wire and the buried signal cable near the lightning point of the high-speed railway. The desired shielding effect properties with the frequency from dc to 1 MHz can be achieved using this method.

1. INTRODUCTION

Railway signaling systems are primarily made up of signaling cables installed below the ground, rails, and overhead power lines. In recent years, large-scale integrated circuits and low-voltage devices have been widely used in electronic control units. Although significant progress has been made in intelligent technology, the resistance of electronic equipment itself to lightning strikes is much lower than that of traction power supply systems. Therefore, the equipment is more likely to be damaged by lightning surges, resulting in frequent circuit burnout and system failure in the signaling system, and even traffic accidents and casualties in severe cases [1, 2]. Thence, lightning damage to high-speed railway signaling systems can bring great harm and risk to high-speed train operation.

The integrated grounding system is one of the important systems for lightning protection of high-speed railways as a discharge channel for large currents [3]. The comprehensive grounding system of high-speed railways in China is mainly composed of through-ground wires, grounding devices, and grounding connecting wires. In actual construction, the outdoor signaling cables are usually laid in the

Received 25 August 2022, Accepted 27 October 2022, Scheduled 9 November 2022

* Corresponding author: Zhiguo Liang (LZG5571@163.com).

[1] Postgraduate Department, China Academy of Railway Sciences, Beijing 100000, China. [2] Signal & Communication Research Institute, China Academy of Railway Sciences, Beijing 100000, China. [3] Key Laboratory of Opto-Electronic Technology and Intelligent Control, Ministry of Education, Lanzhou Jiaotong University, Lanzhou 730000, China.

same groove as the through-ground wires or placed above them. Moreover, both the signaling cable and other trackside equipment, including the trackside equipment of strong current professionals, should be connected to the through ground wire [4] laid along the railway line to ensure that the potential between pieces of equipment is equal. When lightning strikes the overhead contact wire or pillar, most of the lightning current will flow through the grounded terminal to the through-ground wire [5], where it will be dissipated by propagation. This case makes the buried signaling cable laid along the railway line, which is the main channel for coupling electronic equipment with lightning electromagnetic pulses. The lightning electromagnetic wave running across the through-ground wire will generate overvoltage and overcurrent surges on the signaling cable and damage the electronic equipment connected to it [1]. It will also damage the insulation of the cable or interfere with transmission data. The electromagnetic interference on the buried signaling cable should attract sufficient attention. Unfortunately, on the one hand, studies focusing on coupled lightning electromagnetic pulses on buried signaling cables in recent years are limited [6]. On the other hand, according to the safety management regulations, organizing practical experiments during train operation is impossible, so relevant experimental data are lacking. Considering the lack of quantitative analysis of underground lightning induction, we cannot propose economic and effective solutions for lightning protection of outdoor signaling cables and their terminal electronic equipment. A suitable theoretical modeling approach can give us quantitative insight into the spatial electromagnetic field distribution of the through-ground wire under the lightning current impact and its coupling effect on buried signaling cables. This forms the genesis of the present work.

Typically, the study of the induction calculation and influencing factors of the cable coupled lightning electromagnetic field, including buried cables [7–10] and overhead transmission lines (TLs) [11–14], is carried out using the field-to-TL coupling model. In addition, two research approaches have been applied to realize it in the literature: the TL theory [15–17] and the full-wave approach based on the solution of Maxwell's equations [11, 18]. Both methods can be used to assess the induced voltage and current on the signaling cable within the propagation range of lightning electromagnetic wave. However, according to the research purpose of this study, a more effective calculation method should be selected. The voltages and currents at any point along the cable can be obtained directly through the TL solution. By contrast, the full-wave approach can only be obtained by spatial integration. The reason is that the full-wave method is based on Maxwell's equations, which can only obtain the induced electric field and induced magnetic field in space. However, all the electromagnetic and electric fields propagating into the air and soil have been converted into their corresponding line impedance and line conductance in the TL method. A frequency domain solution is particularly advantageous when considering the propagation paths of different media and the frequency dependence of soil electrical parameters in the coupling model. Meanwhile, the calculation method of the full-wave solution of Maxwell's equations allows for an integrated modeling of the entire electrical system including the conductors, excitations, and respective grounding works. This modeling approach has the advantage of simultaneously considering the electromagnetic induction of lightning and conductive coupling. Given the above, using TL equations directly is difficult, whereas full-wave Maxwell's equations would be a considerably better alternative for studying frequency-dependent features in the frequency domain.

This work aims to evaluate the electromagnetic interference of buried signaling cables exposed to the lightning electromagnetic field environment and provide the necessary reference for the development of railway lightning protection technology in China. In this paper, the coupling impact of the through-ground wire on the signaling cable buried in the lossy dispersive soil under the excitation of lightning current is evaluated using a full-wave technique based on FEM solutions to Maxwell's equations. The rest of the paper is further organized as follows. Section 2 briefly presents the use of finite element modeling to calculate lightning electromagnetic fields and induced currents, including the through-ground wire excited by lightning current, examined signaling cable, and their respective grounding systems. Section 3 describes the numerical results for each situation, as well as analysis and discussion. Finally, in Section 4, concluding remarks are provided.

2. SYSTEM UNDER STUDY AND MODELING GUIDELINES

Relative locations of pillar foundation, through-ground wire, buried signaling cable, and grounding terminal are shown in Figure 1.

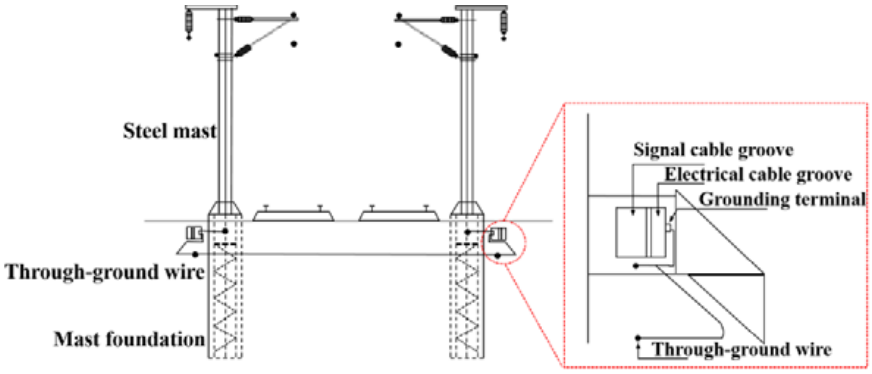

Figure 1. Schematic diagram of the line structure of the subgrade section of the passenger-dedicated railway line.

The comprehensive grounding system of the subgrade section of the high-speed railway is a three-dimensional grounding network composed of protective lines, steel rails, through-ground wires, and overhead contact wire pillars. The underground part of the system buried in the soil includes through-ground wires and contact wire pillar foundations, as shown in Figure 1. According to the construction principle, the contact wire pillars are laid along the railway line at an interval of 50 m, and vertically into the ground for 3 m. The through-ground wire is generally positioned 0.4 m below the top surface of the track-bed on both sides of the railway, which is connected to the integrated grounding system by lead wires, crimping pieces, and grounding terminals. The signaling cables connecting the electronic units in the mechanical room and the trackside electronic units are installed 0.2 m above the through-ground wires and laid in parallel along the railway lines with the through-ground wires [4].

To focus on the fundamental aspects regarding the coupling of transient electromagnetic field on the underground signaling cable, the through-ground wire is excited by the lightning current under extreme conditions according to the research goal of this study. Therefore, the modeling is carried out according to the above actual construction requirements, and the following situations are considered: when the lightning strike occurs near the grounding terminal reserved on the ground by the comprehensive grounding system of the subgrade section, the lightning current invades the through-ground wire in the unreinforced interconnection area, and only the lightning current in the grounding conductor suffering from a lightning strike is considered, ignoring the lightning channel current.

The next sections detail the models adopted for each component of the system.

2.1. Mathematical Model of the Lightning Current

In the study of triggering lightning events, the lightning return stroke current waveforms measured by scholars can be well expressed by the analytical representations using the sum of two Heidler functions [7]. Thus, in this study, the lightning current is mathematically characterized using the Heidler function, which models a lightning pulse [19], making it suited for expressing a phenomenon that undergoes a quick change as its value increases, followed by a slow variation during the decrease of its waveform.

$$i = \frac{i_{\max}}{\eta} \frac{(t/\tau_{11})^n}{1 + (t/\tau_{11})^n} \exp\left(-\frac{t}{\tau_{12}}\right) \tag{1}$$

The adopted parameters which are listed in Table 1 were used for the first stroke and the negative subsequent stroke, according to IEC 61312-1 [5]. Based on [20], the spectrum function calculation of lightning waveform is realized for the subsequent study of lightning impulse response in the frequency domain. The considered configuration is shown in Figure 2.

Table 1. Heidler parameters for first and subsequent strokes [14].

Parameters	the front duration (μs)	the time to half value (μs)	$i_{\max}$ (kA)	τ_{11} (μs)	τ_{12} (μs)	η	n
First stroke	10	350	200	19	485	0.930	10
Subsequent stroke	0.25	100	50	0.454	143	0.993	10

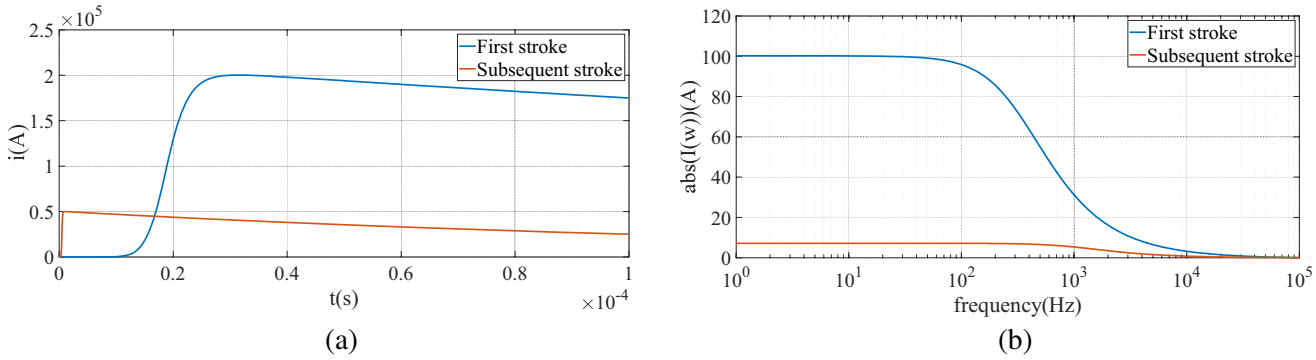

Figure 2. Heidler lightning current function model. (a) The function in the time domain; (b) The magnitude of its Fourier transform.

2.2. Model for Frequency-Dependent Soil Parameters

As pointed out in [21, 22], in any given frequency range, the conductivity and relative permittivity of soil reveal frequency dependence. To verify, the authors of the above papers tested and simulated the reaction of electrodes buried in the soil to currents with lightning waveform patterns. The results show that the experimental results are in good agreement with the simulation considering frequency variation characteristics. In the following work, we will consider whether ignoring this frequency dependence will lead to considerable inaccuracies in the findings.

According to Maxwell's equations, the process of lightning current dispersion in soil medium through the through-ground wire can be described by the full current law of time-varying electromagnetic field [21].

$$\begin{aligned}\overrightarrow{\nabla} \times \overrightarrow{H} &= \sigma_0 \overrightarrow{E} + j\omega(\varepsilon_{real} - j\varepsilon_{imag})\overrightarrow{E} \\ &= (\sigma_0 + \omega\varepsilon_{imag})\overrightarrow{E} + j\omega\varepsilon_{real}\overrightarrow{E} \\ &= \sigma\overrightarrow{E} + j\omega\varepsilon_{real}\overrightarrow{E}\end{aligned} \tag{2}$$

where $\overrightarrow{H}$ and $\overrightarrow{E}$ are the intensity of magnetic field and electric fields in the soil, respectively; $\omega = 2\pi f$ is the angular frequency of grounding current; σ_0 is the low-frequency conductivity of the soil; $\sigma = \sigma_0 + \omega\varepsilon_{imag}$ is the effective conductivity of the soil; $\omega\varepsilon_{imag}$ is polarization losses. Therefore, to correctly evaluate the electromagnetic field intensity in the soil space where the buried signaling cable is located, the frequency-dependent behavior of the electrical soil characteristics must be taken into account in the assessment.

In [21], Visacro and Alipio used the composite electromagnetic model combined with experimental measurement and analytical calculation. According to the measured results, the function analytic formula of soil electrical parameters varying with frequency was derived. This frequency variation formula can better reflect the real characteristics of soil electrical parameters. Therefore, these analytical formulae are used as reference data in this work to describe the soil dispersive feature. These formulae read,

$$\rho(f) = \rho_0 \left\{1 + \left[1.2 \times 10^{-6} \times \rho_0^{0.73}\right] \times \left[(f - 100)^{0.65}\right]\right\}^{-1} \tag{3}$$

$$\varepsilon_r(f) = 7.6 \times 10^3 \times f^{-0.4} + 1.3 \tag{4}$$

The analytical formula obtains reliable results in a wide range of low-frequency resistivity, from 60 to 9100 Ω·m. Typical curves associated with the frequency dependence of the soil relative permittivity and resistivity are shown in Figure 3. In the above expressions, ρ and ε_r are, respectively, the soil resistivity and relative permittivity at the frequency f, ranging from 100 Hz to 4 MHz, and ρ_0 is the low-frequency soil resistivity at 100 Hz.

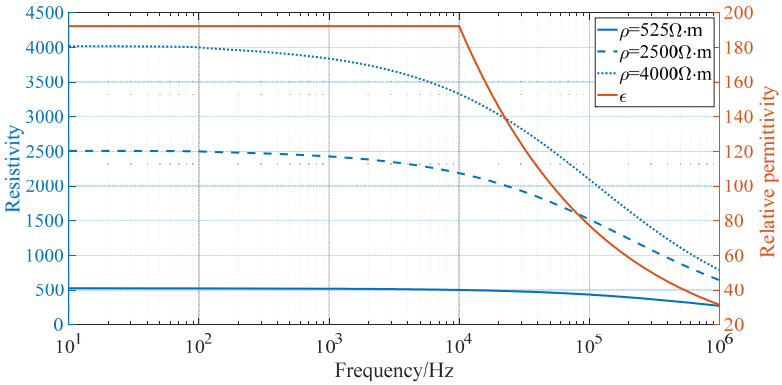

Figure 3. Curves representing resistivity and relative permittivity as a function of frequency.

2.3. Model for the Signaling Cable Buried in the Ground

The cable modeled in this article is a twisted pair cable, buried under the ground surface. The cross-section and model geometry of the cable are shown in Figure 4. Notably, to simplify the simulation, we will ignore the influence of insulation and sheath on the results and focus on the induction effect of the cable shield and inner conductor. The radius of the inner conductor is very small in our modeling in comparison to the mesh size. Referring to the similar method used in the literature [7], the cable shield and inner conductor were assumed to be perfect electric conductors (PECs) [23] in simulations.

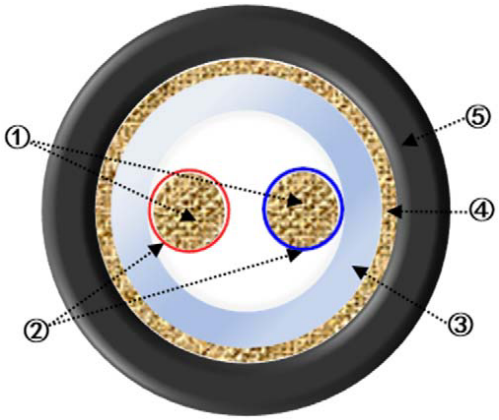

Figure 4. Cable cross section (1 — phase conductors, 2 — phase insulation, 3 — inner insulation, 4 — braided shield, 5 — sheath).

2.4. Electromagnetic Environment Simulation Model

When lightning damage occurs in railway signaling equipment, lightning protection measures and the selection of the defense equipment are often implemented through continuous trial and error.

Considering the contingency of the lightning stroke and given that organizing field tests during train operation is impossible, conducting a comprehensive quantitative analysis of lightning induction on buried signaling cables during lightning stroke is difficult. To overcome the above difficulties, the simulation dates meeting the actual application conditions can be obtained by using the numerical solution method [24, 25].

To calculate the lightning electromagnetic fields and the induced currents on the cable shield, we use a full-wave method based on FEM. The electromagnetic environment simulation model established in COMSOL Multiphysics 5.6 is shown in Figure 5, and the frequency domain is analyzed. Using this method, we can calculate the electromagnetic infield that the buried signaling cable is located in two-dimensional and three-dimensional spaces. RF module's electromagnetic-wave (EMW) solver is based on the finite-element solution of the weak-form representation of the frequency-domain vector wave equation, which is employed in our simulations [26]. This module enables the introduction of frequency dependence of soil electrical parameters and the frequency domain form of the lightning wave to the analyzed model. When the finite-element approach is used in the open region of the model, a perfectly matched layer (PML) is necessary to prevent waves from being reflected by the boundaries. Representative conditions were assumed in the model for lightning current waveforms and cable parameters, as discussed in the above sections.

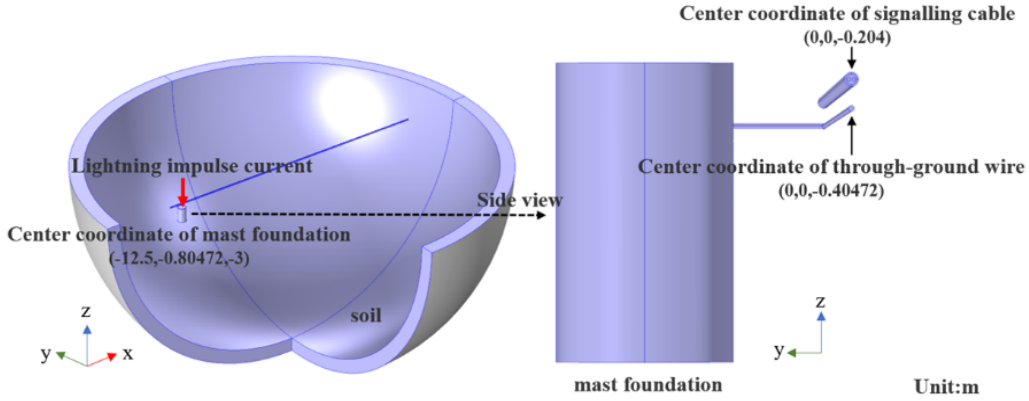

Figure 5. Relative position of the mast foundation, signaling cable, and through-ground wire.

The formulas for modeling are based on Maxwell's equations, and they also follow material laws with propagation in numerous media. The governing equations for evaluating lightning electromagnetic fields could be rigorously established according to the second-order vector wave equation.

$$\overrightarrow{\nabla} \times \left(\mu_r^{-1} \overrightarrow{\nabla} \times \overrightarrow{E}\right) - \omega^2 \left(\varepsilon_r - j\frac{\sigma}{\omega}\right) \overrightarrow{E} = 0 \tag{5}$$

where $\overrightarrow{E}$ (V/m) is the electric field vector; μ_r, ε_r, and σ mean the relative permeability, relative permittivity, and electric conductivity of a given medium, respectively; and ω is the angular frequency.

The electric field is given by Eq. (5). The magnetic field strength H (A/m) at an arbitrary observation point in free space is given by the following equation:

$$\overrightarrow{\nabla} \times \overrightarrow{E} = -j\omega\mu_0\mu_r H \tag{6}$$

Having obtained the components of the electric and magnetic fields with reference to the above formulas, at any given frequency, the induced voltage and induced current along the line are calculated by the integral form of Ampere's equation.

3. NUMERICAL RESULTS

3.1. Validation of the Model

We need to test the accuracy of using the FEM to calculate the electromagnetic field coupling to the TL first. Paknahad et al. [24] have completed this work. According to the actual test environment of

the International Center for Lightning Research and Testing (ICLRT) at Camp Blanding, Florida, the authors used the FEM to calculate the induced current on a buried coaxial power cable and compared the results with the measurement data presented in [24]. The authors found that if the electrical parameters of the soil in the model are close to those of the real test soil, then the calculated results correspond well with the measured waveform. This conclusion has also been verified by Paulino et al. [27]. Therefore, the FEM based on Maxwell's equations can accurately solve the problem of electromagnetic field coupling to TL. This article will not repeat the verification work.

3.2. Analysis of Underground Lightning Electromagnetic Fields

To evaluate the lightning induction effect on buried signaling cables, the electromagnetic field distribution near the lightning current discharge channel in soil should be evaluated when the through-ground wire is used as the transmission channel of the lightning current firstly. As an air-soil interface near the through-ground wire exists, the influence of its existence on the electromagnetic field distribution also needs to be considered.

In the RF module of COMSOL multi-physics software, the lightning strike position is assumed to be located at the grounding terminal of the contact wire pillar foundation. Ignoring the shunt effect of the pillar, all lightning current will flow through the through-ground wire. The through-ground wire, with a radius of 0.00472 m and a distance of dm below the ground, is established. The air and soil domains with a radius of 0.05 m are also considered. Air and soil domains are set as a perfect matching layer with a thickness of 0.005 m respectively to simulate the edges of a commutation domain. The geometric dimensions of the model are shown in Figure 6. We analyze the lightning electromagnetic fields from different induction angles, respectively, at P1, P2, and P3, as shown in Figure 6.

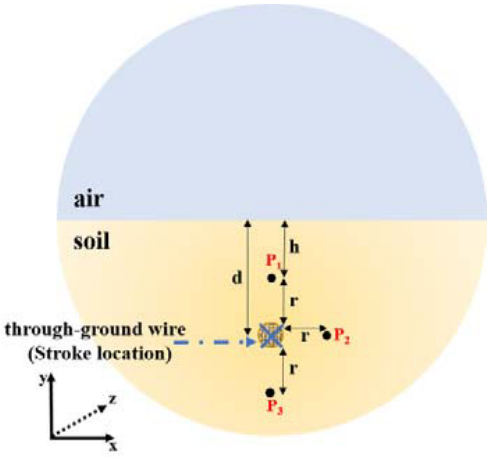

Figure 6. Geometry for the calculation of lightning electromagnetic fields below the ground.

Figures 7–10 show the simulated electromagnetic field at three observation points below the ground with the same distance from the lightning strike point when the first lightning strike hits the through-ground wire. As shown in these figures, the air-soil interface and the distance from the lightning strike point have a significant effect on all the components of the lightning electromagnetic fields. The conclusions that may be drawn as follows:

1) For the horizontal electric field (Figure 7), when the air-soil interface exists in space, the effect of the soil stratification prevails. When the distance between observation point P1 and the lightning striking point is the same, the closer it is to the air-soil interface, the smaller the electric field intensity is. The electric field intensity of the observation point is inversely proportional to the distance from the lightning point, which is consistent with the definition of the electric field intensity. The air-soil interface can be regarded as a structure in which the conductivity of the upper layer is more than that of the lower layer. Therefore, the conclusion of the electric field strength and the

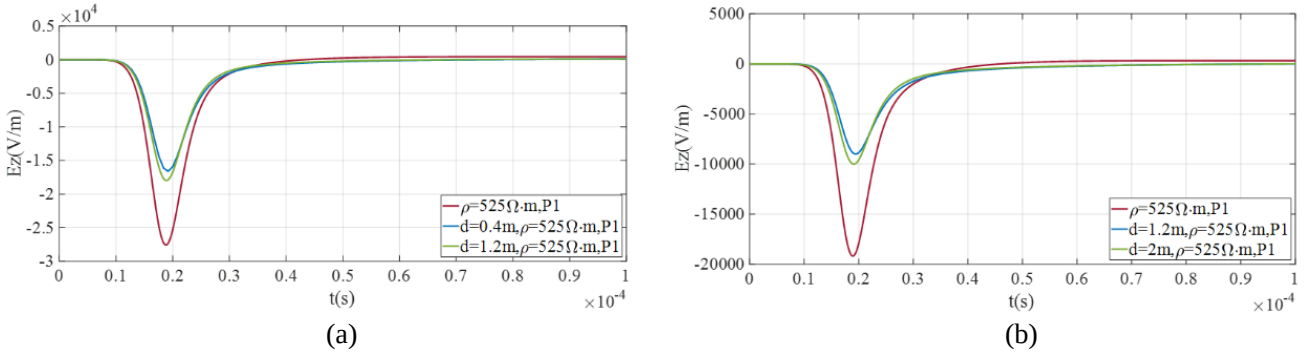

Figure 7. Horizontal components of the electric field (E_z) at observation point P1 for the case of soil resistivity $\rho_{soil} = 525\,\Omega{\cdot}\mathrm{m}$. (a) $r = 0.2\,\mathrm{m}$, (b) $r = 1\,\mathrm{m}$. Red line: far away from the air-soil interface ($d = \infty$).

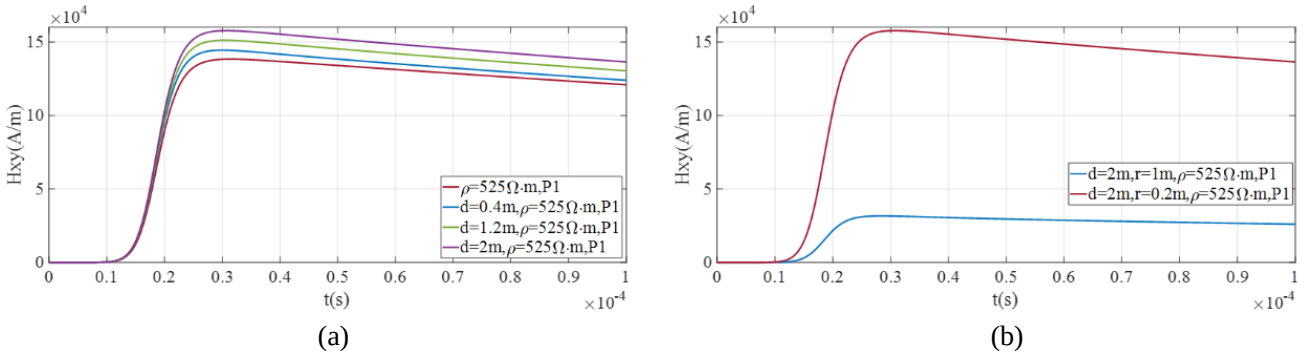

Figure 8. Magnetic field ($H_{x\text{-}y}$) at observation point P1 for the case of soil resistivity $\rho_{soil} = 525\,\Omega{\cdot}\mathrm{m}$. (a) $r = 0.2\,\mathrm{m}$. Red line: far away from the air-soil interface ($d = \infty$), (b) $d = 2\,\mathrm{m}$.

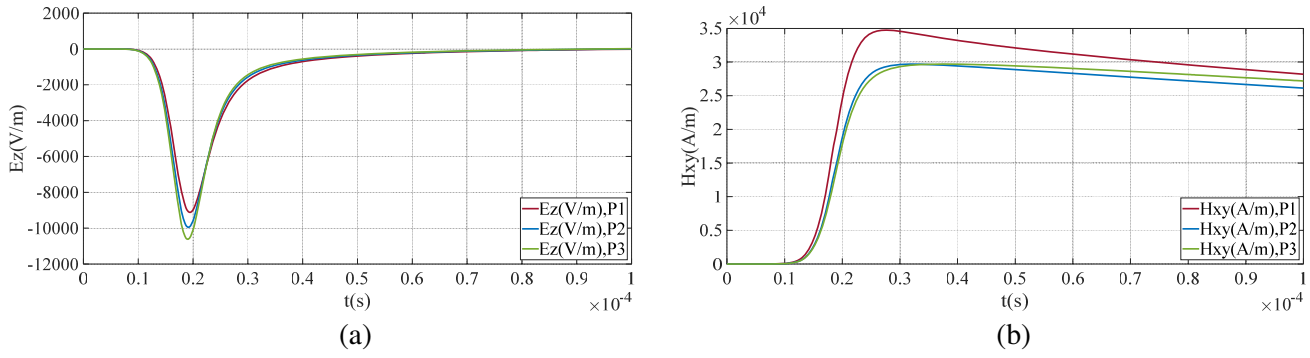

Figure 9. E_z and $H_{x\text{-}y}$ at observation point P1, P2 and P3 for the case: (1) soil resistivity $\rho_{soil} = 525\,\Omega{\cdot}\mathrm{m}$; (2) $r = 1\,\mathrm{m}$, $d = 1.2\,\mathrm{m}$.

following conclusion of magnetic field strength can also be used to analyze other layered structures with different conductivities.

2) When air-soil stratification exists in space, the closer it is to the air-soil interface, the smaller the magnetic field strength is at observation point P1 with the same distance from the lightning striking location (Figure 8). However, when the lightning point is very far away from the air-soil interface, the magnetic field intensity is smaller, which is an interesting conclusion.
3) The influence of the air-soil interface on the electromagnetic field can also be analyzed in Figure 9. At the same distance from the lightning strike point, the air-soil interface has a significant effect

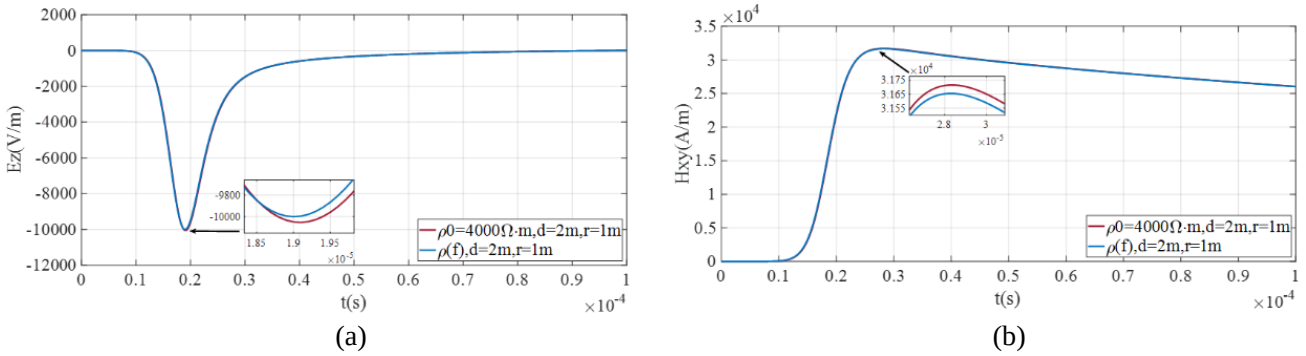

(a) (b)

Figure 10. (a) E_z and (b) $H_{x\text{-}y}$ at observation point P1 for the case: (1) the low-frequency resistivity of soil $\rho_{soil} = 4000\,\Omega$·m, the relative permittivity $\varepsilon = 10$; (2) $r = 1\,\text{m}$, $d = 2\,\text{m}$. Red line: soil with constant resistivity. Blue line: soil with frequency dependent resistivity.

on the lightning electric field. The closer the induced magnetic field is to the layered interface, the stronger the magnetic field strength is.

4) According to Figures 7–9, the results are obtained under the constant soil conductivity. In the following, we can analyze the influence of the frequency dependence of soil resistivity on the electromagnetic field by modeling (Figure 10). To obtain more significant results in the model, the soil low-frequency conductivity is set to $4000\,\Omega$·m. Since the relative permittivity of the soil below 10 kHz is suggested at 192 [21], which is given by Eq. (4) at 10 kHz. Therefore, the frequency variation effect of the soil relative permittivity is ignored and set to 192. The findings suggest that the frequency-dependence of soil conductivity contributes to the reduction of electromagnetic field intensity in high resistivity soils. However, owing to the close proximity of the observation point to the lightning strike location, the frequency-dependence of soil conductivity has a negligible influence on the electromagnetic field intensity values.

3.3. Lightning Coupling Analysis on Buried Signaling Cables

In this part, the evaluation of the electromagnetic coupling at the buried signaling cable is carried out when the lightning current flows through the through-ground wire of the unreinforced interconnection area. The model of this study is shown in Figure 5, and the sizes of the simulation are described in Figure 11. The length of the signaling cable and the through-ground wire are assumed to be both 25 m, which is half of the distance between the two pillar foundations. The signaling cable and through-ground wire are laid in parallel, with 0.2 m and 0.4 m below the air-soil interface, respectively. One of the signal cable cores is grounded at both ends. G and H represent the grounding resistance, and the resistance value is $50\,\Omega$, respectively. E and F represent the grounding impedances at the two ends of the cable shield. Different grounding conditions can be achieved by configuring different E and F values. To simplify simulations and discussions, the cable shield is assumed to be solid tubular with no magnetic field leakage. In all simulations, different situations are considered to provide a comprehensive analysis of the electromagnetic coupling on the signaling cable.

In the above section, in the absence of the signaling cable, the frequency-dependent characteristics of soil have no significant effect on the electric field strength E_z and the magnetic field strength $H_{x\text{-}y}$ in the space near the through-ground wire. However, the air-soil interface has a significant effect on them. It is well known that the induced current is calculated by integrating the magnetic field strength H around the cable in a circular route. The magnetic field around the signaling cable is the sum of the electromagnetic field produced by subsurface lightning and the field produced by the charge and current induced on the cable. As a result, a three-dimensional model should be established to quantitatively analyze the induction effect on the signaling cable.

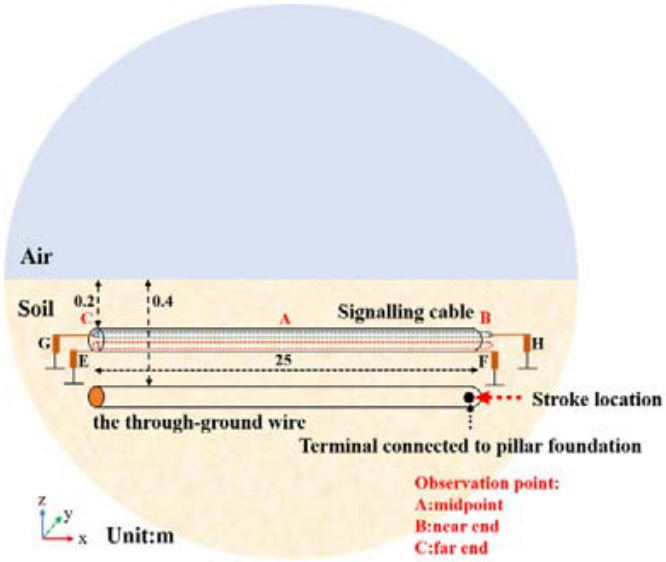

Figure 11. Adopted modeling configuration.

3.3.1. Analysis of Different Soil Resistivity

To evaluate the influence of soil electrical parameter frequency-dependency, a number of situations, including both constant and frequency-dependent parameters, are explored. For electrical parameters, the soil is supposed to have conductivity σ_0 and a relative permittivity ε_r. These parameters are also used in Eqs. (3) and (4) for the case in which the soil is assumed to be frequency-dependent. The analysis is done for three different soil resistivities: $\rho = 525\,\Omega \cdot \mathrm{m}$, $\rho = 4000\,\Omega \cdot \mathrm{m}$, and $\rho(f)$. The low-frequency soil resistivity of $\rho(f)$ is $4000\,\Omega \cdot \mathrm{m}$. In all three cases, we have assumed the same relative permittivity $\varepsilon_r = 192$, and the reason has been explained above and will not be detailed here. The modeling work is carried out based on the following assumptions: (1) The frequency content considered is assumed to be in the range of dc to 1 MHz. (2) The cable shield is well grounded at both ends, and the grounding impedance is set to $0.5\,\Omega$.

The induced voltages in the shield along the cable in soils with different resistivity are shown in Figure 12. The induced currents on the cable shielding layer and cable core respectively are shown in Figure 13. From the results of Figure 12 and Figure 13, evidently, the influence of the frequency dependence of soil electrical parameters on the coupling results generated by lightning electromagnetic field can be ignored when the cable is close to the lightning point.

When both ends of the shield are grounded well, the maximum voltage peak at the endpoints of the shielding layer is $2.38 \times 10^4\,\mathrm{V}$, but the polarity is different. However, the maximum voltage peak is only 1120 V at the cable's center. This voltage distribution is because of the current induced in the conductors of the shield (Figure 13(a)), which will circulate in the circuit formed by the shielding layer and the soil. Therefore, the impedance component along the shield should be considered the distributed, resulting in that each point on the shield will have a different voltage. Owing to the grounding resistances at both ends of the shield being equal and the circuit's reflection coefficient being considered zero, the induced voltage waveforms on either side of the midpoint of the shield are similar, but with opposite polarities. Through the transmission impedance between the shielding layer and cable's inner conductor, the lightning electromagnetic field may generate electromagnetic coupling to the cable core [28], causing serious interference to sensitive equipment connected at both ends of the cable. Notably, the shield transfer impedance is frequency dependent [28, 29]. Therefore, the shielding effectiveness of the shielding layer of the same material and structure is different for different external interference signals.

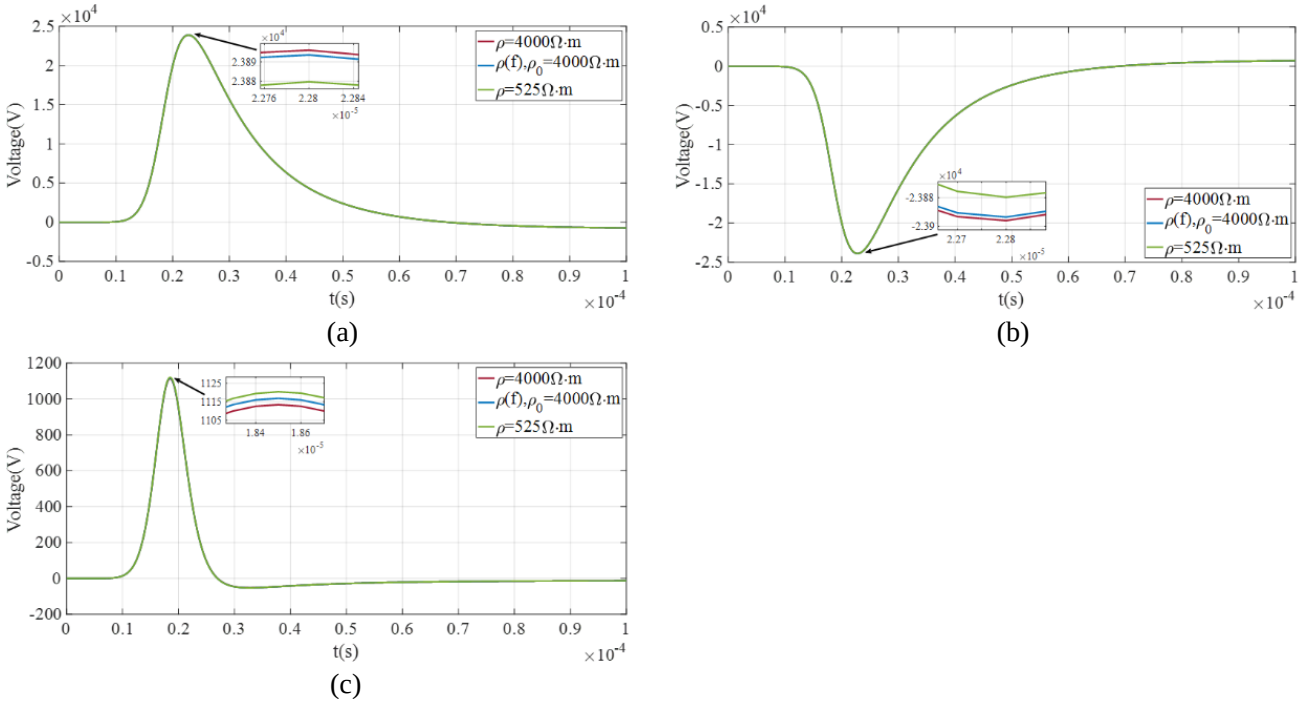

Figure 12. Voltage induced in the shield along with the cable. (a) and (b) at either ends; (c) at midpoint.

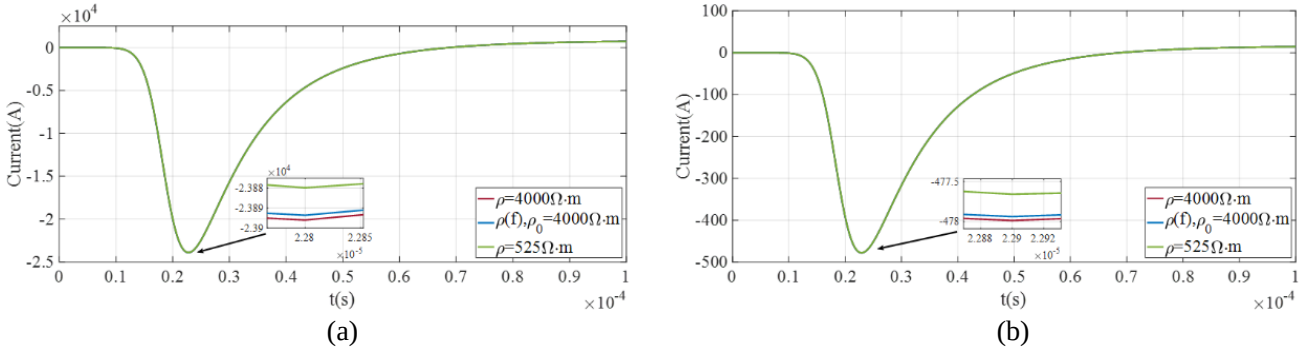

Figure 13. Induced current along the cable. (a) Shield; (b) Core.

3.3.2. Analysis for Different Current Pulse

Considering that the subsequent stroke current has more high-frequency components than the first stroke current, whether the frequency dependency of soil electrical characteristics is more pronounced for the subsequent stroke current should be investigated. In the following, we will use the subsequent stroke current as the excitation for the model while keeping the model setup conditions unchanged. To this aim, we set the parameters of the subsequent stroke current according to Table 1, where $i_{\max}$ is consistent with the first stroke current, both of which are 200 kA.

As shown in Figure 14, the cable core induces a maximum current of 730 A when the through-ground wire is subjected to the subsequent stroke current pulse. The rising time is comparable to that of the lightning current. The induced current in the cable core is characteried by a half-peak width of approximately 7.925 µs, which is significantly shorter than that of the subsequent stroke current (approximately 99.5450 µs). However, the zero-to-peak rise time of the current induced in the cable core is approximately 1.1 µs, which is not much different from the time of the incident current (approximately

1 μs).

Similarly, when the excitation is changed to the first stroke current pulse, the current induced in the cable core reaches a peak value of 478 A. The induced current in the cable core is characterized by a half-peak width of approximately 15.18 μs, which is also much smaller than the impulse current (approximately 350.4 μs). Different from the result when the subsequence stroke current pulse is used as the impulse current, the time of current induced in the cable core from zero to peak is approximately 22.9 μs, which is 8.5 μs ahead of the time of the first stroke current. These results indicate that it will take more time for the induced current in the cable to reach the peak under the subsequence stroke current. The above conclusion is not difficult to understand. With the increase of the soil conductivity, the transverse component of the induced field in the soil gradually expands, resulting in more time for the induced current in the cable to reach the peak. Hence, one can see that the subsequent stroke current displays a stronger frequency dependency of the soil electrical parameters.

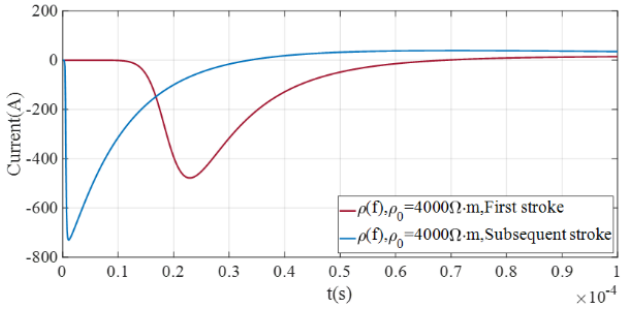

Figure 14. Induced current along with the cable core (the through-ground wire under the action of different lightning currents).

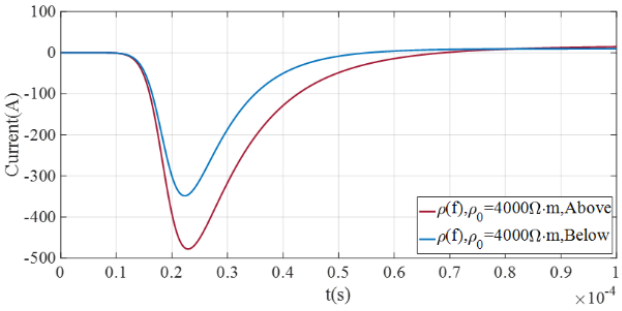

Figure 15. Induced current along the cable.

3.3.3. Analysis of Different Distances between Signaling Cable and Air-Soil Interface

In the previous sections, we discussed the influence of the air-soil interface on the electromagnetic field in soil space. However, the results presented above are obtained without considering the presence of TL near the through-ground wire. According to the construction requirements of the railway signaling equipment, the buried signaling cable is very close to the air-soil interface, and the buried depth is generally not more than 1 meter. Therefore, the study of the influence of the air-soil interface on the induced current cannot be ignored.

On the premise of keeping the relative distance between the through-ground wire and the air-soil interface unchanged (0.4 m), we place the signaling cable above and below the through-ground wire, respectively, keeping the distance from the grounding wire at 0.2 m. By comparing the two results, the influence of the air-soil interface on lightning induction of signal cable is analyzed.

Our result in the above figure (Figure 15) is generally consistent with that presented in Figure 9. Observed at different observation points with the same distance from the lightning point, the closer the air-soil interface is, the stronger the magnetic field strength is, and the greater the induced current is in the cable core.

3.3.4. Analysis for Different Grounding Models of Signal Cable Shielding Layer

When the lightning transient electromagnetic field is coupled to the cable shield, a large current will be generated (depending on the coupling type), resulting in transient overvoltage between the internal conductor and the cable shield, thereby damaging the sensitive equipment at both ends of the cable. We usually use the method of grounding the cable shield to suppress the interference of the external electromagnetic field. There are three types of grounding: floating grounding, single terminal grounding, and double terminal grounding. For different electromagnetic coupling conditions, the shielding effects

of the three grounding modes are different. How to effectively suppress the interference of lightning electromagnetic pulse needs our in-depth study.

The electromagnetic field distribution in the shield and the internal conductor of the cable with different grounding modes are shown in Figure 16. The specific range of the electromagnetic field value is shown in Table 2. Then, Figure 16 shows that the electric field intensity in the shield is mainly distributed near the through-ground wire, with a small difference between the internal conductor and the shield. When the shield of the cable is grounded at both ends, the maximum electric field strength in the cable core is 31% of that using the other two grounding modes. The influence of the grounding modes on the magnetic field distribution of cable is more significant. The maximum magnetic field intensity in the right cable core is 45.4% of that using the other two grounding modes when the shield is grounded at both ends. The maximum magnetic field intensity in the left cable core is 69.9% of that using the other two grounding modes. Therefore, whether both ends of the internal conductor are grounded or not, the double-ended grounding design of the shield can reduce the magnetic field coupling of the external lightning electromagnetic field on the inner conductor of the cable.

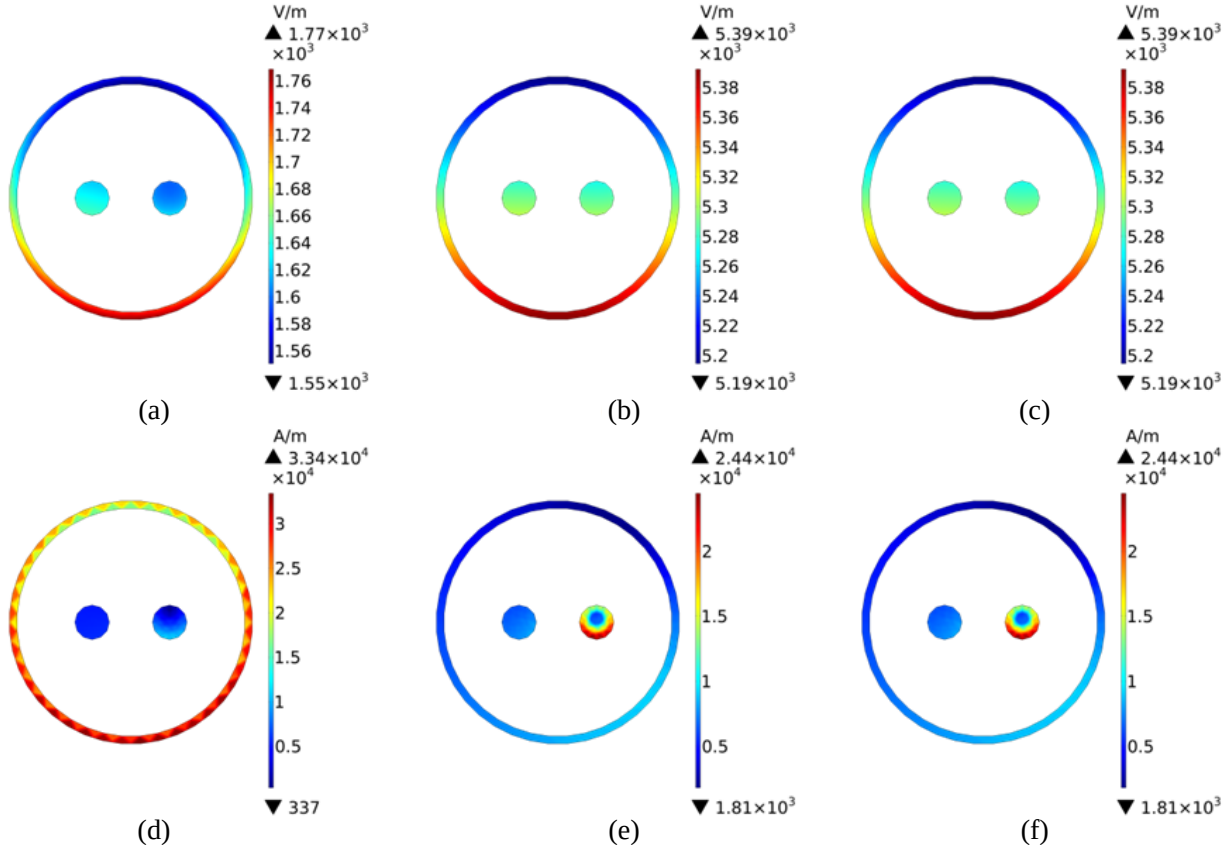

Figure 16. Distribution of electric field strength in a cross-section of the cable near lightning strike point: (a) double-terminal grounding; (b) single-terminal grounding; (c) floating grounding; Distribution of magnetic field strength in a cross-section of cable near lightning strike point: (d) double-terminal grounding; (e) single-terminal grounding; (f) floating grounding; the core of the cable (left): floating on the ground; the core of the cable (right): the double terminal impedance adopt 50 Ω resistance.

All of the above are consistent with the theoretical analysis results. When the shield is grounded at both ends, the shield forms a loop with the soil, and most of the interference current will flow to the soil through the grounding resistance, thus reducing the electric field coupling of the lightning electromagnetic field to the signal cable. In the case of magnetic field coupling, the cable core with both ends grounded is taken as the analysis object first. When the shield is grounded with both ends,

Table 2. Characteristics of the analyzed model.

Grounding mode	Cable core		Cable shield	
	Electric field values (kV/m)	Magnetic field values (kA/m)	Electric field values (kV/m)	Magnetic field values (kA/m)
Double-ended grounding	1.6–1.65	0.337–11.1	1.55–1.77	16.4–33.4
Single-ended grounding	5.27–5.31	6–24.4	5.19–5.39	1.8–9.4
Floating grounding	5.27–5.31	6–24.4	5.19–5.39	1.81–9.4

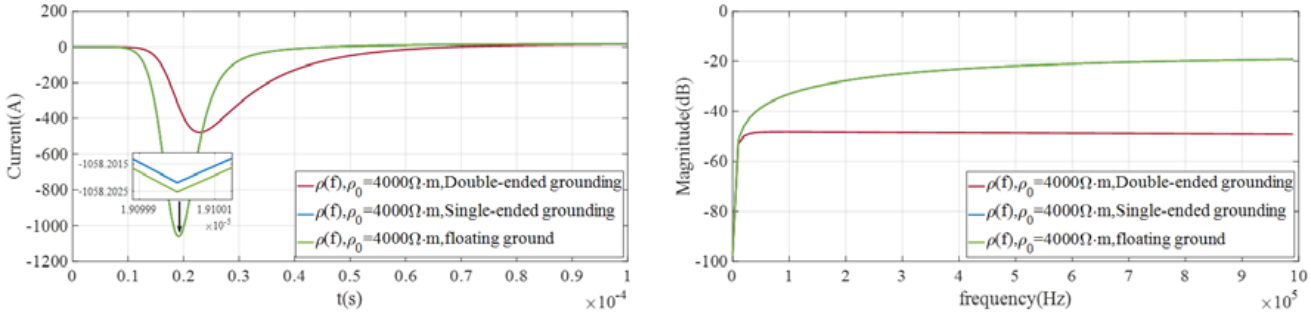

(a) (b)

Figure 17. Analysis for different grounding modes of signal cable shield. (a) Induced current in cable core; (b) Crosstalk coupling coefficient.

the equivalent area of the receiving circuit composed of the cable core and the soil is the smallest, so is the induced current. The induced current in the cable core is shown in Figure 17(a). Next, we take the case of the cable core with two ends floating to the ground into account. The area of the receiving loop composed of the cable core and the soil is very small and can be ignored at low frequency. When the shield is grounded at both ends, unnecessary magnetic field coupling will be introduced. With the increase of the frequency, the capacitive reactance between the cable core and the soil decreases, and the cable core will have the effect of grounding. At this time, the shield with both ends grounding will have a good shielding effect. Crosstalk coupling coefficient (unit: dB) is used to describe the coupling level of the lightning electromagnetic pulse to the cable core (the load at both ends is 50 Ω) under different grounding modes of the shield. Figure 17(b) shows the calculation results. When the frequency range is 0–10^4 Hz, the coupling levels of the three grounding modes are the same. When the frequency range is up to 10^4–10^6 Hz, the coupling coefficient of the double-ended grounding of the shield is significantly less than that of the other two modes.

4. CONCLUSION

In this study, a full-wave finite-element-based solution of Maxwell's equations is performed to evaluate the lightning radiated electromagnetic fields generated from the through-ground wire stroked by the lightning current. We have also discussed the simulation results for lightning-induced currents and voltages on the buried signaling cable. We further analyzed the various factors affecting field-to-TL coupling. The adopted model is able to take the frequency dependence of the soil electrical parameters into account, which is usually neglected in the previous calculation of the field-line coupling in high-speed railways. The numerical analysis and discussion carried out in this study allow us to draw the following conclusions:

1) The lightning electromagnetic fields below the ground are significantly affected by the air-soil interface. The horizontal electric field at the observation point 0.2 m below the lightning current injection point reaches a peak value of 1.06×10^4 V/m. When the lightning current flows through

the through-ground wire with 0.4 m depth far from the ground, it is 1.505×10^3 V/m higher than the upper observation point (9.115×10^3 V/m) at the same distance from the injection point. The calculation result of the vertical component of the magnetic field is just the opposite. The peak value above the injection point is 3.47×10^4 A/m, which is higher than that below (2.95×10^4 A/m). However, the frequency dependence of soil resistivity has little effect on lightning electromagnetic field. The specific influence is related to the high-frequency component of the lightning current wave, the distance from the lightning point, and the low-frequency resistivity of soil.

2) Simulations show that the coupling strength of the lightning electromagnetic field to the buried signaling cable is greatly affected by the parameters such as wave shape of lightning current, soil resistivity, the distance between the cable and the air-soil interface, and the distance between the cable and the lightning strike point. It was highlighted that the smaller the front duration of the lightning wave is, the more significant the influence of frequency dependence of soil electrical parameters is on the induced current of the cable. Additionally, we noticed that the closer the lightning strikes are, the greater the generated currents are on the buried wire. The air-soil interface will also affect the cable's induced current. Although the distance between the cable and the air-soil interface increased by only 0.4 m, the induced current on the cable core decreased by 27.2%. In the design of lightning strike protection, the most severe inductive situations should be considered.
3) At the end of this study, we compare the shielding grounding methods commonly used in cable protection. For double-ended grounding of a single-layer, the desired shielding effect properties with the frequency from 0 to 10^6 Hz can be achieved. However, in engineering practice, comprehensively considering the working frequency (or easily disturbed frequency) of the sensitive circuit connected to the two ends of the signaling cable and the grounding mode of the sensitive circuit is still necessary. Based on these considerations, the most suitable signaling cable protection measures are designed.

In summary, this study aims to minimize the electromagnetic field coupling between the through-ground wire and the signaling cable near the lightning strike point. The above research provides not only quantitative analysis data for the protection methods of signaling cables, but also an effective modeling method for electromagnetic interference research of underground cables.

5. CONFLICT OF INTEREST

The authors declare that they have no competing interest.

6. AUTHOR CONTRIBUTIONS

YQ operated the experiment, analyzed the data, and wrote the manuscript. LW, SB and JG operated the experiment. HZ jointed in data analysing and editing. ZL and WD was in charge of the project. All authors contributed to the article and approved the submitted version.

7. FUNDING STATEMENT

This work was supported in part by the Key Project Foundation of China Academy of Railway Sciences Corporation Limited under grant 2020YJ017 and the Scientific and Technical Exploitation Program of China Railway under grant J2021G006.

8. DATA AVAILABILITY STATEMENT

The data used to support the findings of this study are available from the corresponding author upon request.

REFERENCES

1. Luo, L., D. Wang, and M. Hao, "7.23 Yong-Wen line particularly major railway accident investigation report," 7.23 Yong-Wen Line Particularly Major Railway Accident Investigation Team of The State Council, Beijing, 2011.
2. Arai, H., Y. Hizawa, H. Fujita, et al., "Lightning overvoltage of rails and signalling cables in electrified/non-electrified section," *33rd International Conference on Lightning Protection (ICLP)*, 1–6, IEEE, Estoril, 2016.
3. Zhang, B., H. Xue, Z. Jin, et al., "Transient potential distribution of transmission tower and its grounding device under lightning," *High Voltage Engineering*, Vol. 39, No. 2, 393–398, 2013.
4. Ren, R., *Engineering Design Guidelines for Lightning Protection System of Railway Comprehensive Grounding and Signaling Equipment*, China Railway Press, Beijing, 2009.
5. IEC(Iec), IEC 61312-1 Protection against lightning electromagnetic impulse — Part 1: General principles[S], IEC, London, 1995.
6. Papadopoulos, T. A., C. A. Charalambous, A. Dimitriou, et al., "Assessing the inductive electromagnetic interference caused on a railway system 5 by a nearby hvdc underground cable link," *30th CIGRE Greece National Conference "e-Session 2020"*, CIGRE, Paris, 2020.
7. Paolone, M., E. Petrache, F. Rachidi, et al., "Lightning induced disturbances in buried cables — Part II: Experiment and model validation," *IEEE Transactions on Electromagnetic Compatibility*, Vol. 47, No. 3, 509–520, 2005.
8. Petrache, E., F. Rachidi, M. Paolone, et al., "Lightning induced disturbances in buried cables — Part I: Theory," *IEEE Transactions on Electromagnetic Compatibility*, Vol. 47, No. 3, 498–508, 2005.
9. Sunitha, K. and M. J. Thomas, "Effect of soil conditions on the electromagnetic field from an impulse radiating antenna and on the induced voltage in a buried cable," *IEEE Transactions on Electromagnetic Compatibility*, Vol. 61, No. 4, 990–997, 2019.
10. Yang, B., B. H. Zhou, and B. Chen, "Numerical study of lightning-induced currents on buried cables and shield wire protection method," *IEEE Transactions on Electromagnetic Compatibility*, Vol. 54, No. 2, 323–331, 2012.
11. Akbari, M., K. Sheshyekani, A. Pirayesh, et al., "Evaluation of lightning electromagnetic fields and their induced voltages on overhead lines considering the frequency dependence of soil electrical parameters," *IEEE Transactions on Electromagnetic Compatibility*, Vol. 55, No. 6, 1210–1219, 2013.
12. Nematollahi, A. F. and B. Vahidi, "The effect of the inclined lightning channel on electromagnetic fields and the induced voltages on overhead lines," *Electrical Engineering*, Vol. 103, No. 6, 3163–3176, 2021.
13. Paolone, M., F. Rachidi, A. Borghetti, et al., "Lightning electromagnetic field coupling to overhead lines: Theory, numerical simulations, and experimental validation," *IEEE Transactions on Electromagnetic Compatibility*, Vol. 51, No. 3, 532–547, 2009.
14. Silveira, F. H., S. Visacro, R. Alipio, et al., "Lightning-induced voltages over lossy ground: The effect of frequency dependence of electrical parameters of soil," *IEEE Transactions on Electromagnetic Compatibility*, Vol. 56, No. 5, 1129–1136, 2014.
15. Ianoz, M., C. A. Nucci, and F. M. Tesche, "Transmission line theory for field-to-transmission line coupling calculations," *Electromagnetics*, Vol. 8, Nos. 2–4, 171–211, 1988.
16. Nucci, C. A. and F. Rachidi, "Interaction of electromagnetic fields generated by lightning with overhead electrical networks," *The Lightning Flash*, V. Cooray (ed.), 559–610, Institution of Engineering and Technology, Hong Kong, 2014.
17. Rusck, S., "Induced-lightning overvoltages on power transmission lines with special reference to the overvoltage protection of low voltage networks," *Trans. R. Inst. Technol.*, Vol. 120, 1–118, 1958.
18. Napolitano, F., A. Borghetti, C. A. Nucci, et al., "Use of the full-wave Finite Element Method for the numerical electromagnetic analysis of LEMP and its coupling to overhead lines," *Electric Power Systems Research*, Vol. 94, 24–29, 2013.

19. Heidler, F. and J. Cvetić, "A class of analytical functions to study the lightning effects associated with the current front," *European Transactions on Electrical Power*, Vol. 12, No. 2, 141–150, 2002.
20. Vujević, S. and D. Lovrić, "Exponential approximation of the Heidler function for the reproduction of lightning current waveshapes," *Electric Power Systems Research*, Vol. 80, No. 10, 1293–1298, 2010.
21. Visacro, S. and R. Alipio, "Frequency dependence of soil parameters: Experimental results, predicting formula and influence on the lightning response of grounding electrodes," *IEEE Transactions on Power Delivery*, Vol. 27, No. 2, 927–935, 2012.
22. Visacro, S., R. Alipio, M. H. M. Vale, et al., "The response of grounding electrodes to lightning currents: The effect of frequency-dependent soil resistivity and permittivity," *IEEE Transactions on Electromagnetic Compatibility*, Vol. 53, No. 2, 401–406, 2011.
23. Sun, Q., E. Klaseboer, A. J. Yuffa, et al., "Field-only surface integral equations: Scattering from a perfect electric conductor," *Journal of the Optical Society of America A*, Vol. 37, No. 2, 276–283, 2020.
24. Paknahad, J., K. Sheshyekani, F. Rachidi, et al., "Lightning electromagnetic fields and their induced currents on buried cables. Part II: The effect of a horizontally stratified ground," *IEEE Transactions on Electromagnetic Compatibility*, Vol. 56, No. 5, 1146–1154, 2014.
25. Sheshyekani, K. and J. Paknahad, "The effect of an ocean-land mixed propagation path on the lightning electromagnetic fields and their induced voltages on overhead lines," *IEEE Transactions on Power Delivery*, Vol. 30, No. 1, 229–236, 2015.
26. Comsol. RF Module User's Guide 5.6[M]. COMSOL, Kerala, 2019.
27. Paulino, J. O. S., C. F. Barbosa, and W. C. Boaventura, "Lightning-induced current in a cable buried in the first layer of a two-layer ground," *IEEE Transactions on Electromagnetic Compatibility*, Vol. 56, No. 4, 956–963, 2014.
28. Vance, E. F., *EMP Interaction Note: Internal Voltages and Currents in Complex Cables*, Stanford Research Institute, Menlo Park, CA, 1967.
29. Sunde, E. D., *Earth Conduction Effects in Transmission Systems*, Dover, New York, NY, 1968.